CRYSTAL GROWTH & DESIGN

Article

pubs.acs.org/crystal

Coupling between Molecular Mobility and Kinetics of Crystal Growth in a Hydrogen-Bonded Liquid

Alejandro Sanz* and Kristine Niss

"Glass and Time", IMFUFA, Department of Science and Environment, Roskilde University, Postbox 260, DK-4000 Roskilde, Denmark

ABSTRACT: Our aim here is to gain new insight into the nature of the crystalline phase formed in supercooled glycerol near the glass transition temperature and to establish the interrelationship between the kinetics of crystal growth and fundamental dynamic properties. The liquid's dynamics and the crystalline development in glycerol, a hydrogen-bonded liquid, is studied by means of dielectric spectroscopy. We monitored the kinetics of crystallization by isothermal treatment at temperatures between 220 and 240 K (T_g = 185 K). Given the thermal protocol employed, we stimulated the growth of the crystalline phase from pre-existing nuclei, in such a way that the observed kinetics is dominated by the crystal growth step. Our experimental results are discussed in terms of the classical theory of crystallization which predicts a significant correlation between the liquid's diffusion and the crystal growth rate. The coupling between dynamic properties, such as dielectric α relaxation time, viscosity, and self-diffusion coefficient, and the characteristic crystal growth time is analyzed. We find that the crystal growth time scales with the glycerol's self-diffusion coefficient as $\tau_{cryst} \propto D^{-0.85}$, confirming that the liquid's dynamics is the principal factor governing the crystal growth in glycerol above but close T_g.

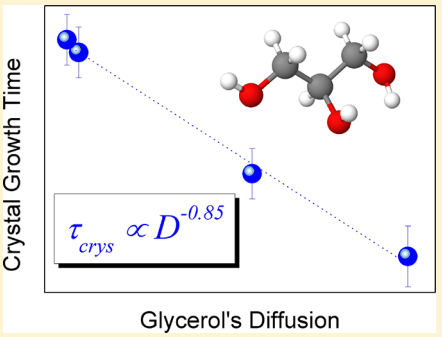

INTRODUCTION

Supercooled liquids, that is, liquids below their melting temperature T_m, have higher values of free energy with respect to the crystalline state. This excess of free energy drives the transformation of liquids into crystals through a first-order phase transition. Crystallization is a complex phenomenon, in which, apart from this thermodynamic driving force, several factors are simultaneously involved. Molecular mobility of the mother phase, surface tension of the liquid/crystal interface, intermolecular attractions, purity of the sample and its interactions with the environment, among others, are known to govern the crystallization tendency of supercooled liquids.[1−6] Indeed, it is well established that the liquid's dynamics plays a major role in the crystalline development, although the exact nature of this interrelationship is still a matter of debate.[1,7,8] Moreover, contrary to the general impression, the study of crystallization may be seen as an indirect strategy for learning more about the relaxation dynamics of supercooled liquids.[2,9,10]

Seeking a better understanding of the structure−dynamics correlations during crystallization, here we report on the crystal growth behavior of the associated liquid glycerol. Glycerol is a model in numerous studies from the glass-forming-system community, and it has also attracted the attention of groups interested in exploring its crystallization behavior.[4,11−14] The present report provides new information about the kinetics of crystal growth above but close to the glass transition temperature, T_g, as explored by dielectric relaxation spectroscopy. We followed the thermal protocol proposed by Möbius and co-workers, who considered the possibility that a glacial phase could be formed near T_g.[12] Our hypothesis is that the transformation of liquid glycerol into a metastable glacial phase (presumably formed by nanocrystals dispersed in a liquid matrix) would lead to the presence of an active dielectric relaxation due to the incomplete molecular ordering. We repeated our experiments several times and, with the exception of one case, we found no evidence of formation of a glacial or partially disordered crystal phase.

The characteristic crystallization time at different temperatures was estimated through the so-called Avrami equation using the method proposed by Avramov and colleagues.[15] The Avramov approach also provided us information about the dimensionality and morphology of the growing crystals. We complemented these results by applying the Maxwell−Wagner model for heterogeneous systems to our dielectric data as it has been recently proposed in a real-time crystallization study.[5]

Finally, we investigate the coupling between the characteristic time of crystal growth and the dielectric α relaxation time and, since we discuss our results under the framework of the classical theory, we also correlate our data with the liquid's self-diffusion coefficient. Our results indicate that the main factor governing the crystallization tendency in supercooled glycerol near T_g is the molecular mobility, at least for the thermal protocol we employed.

EXPERIMENTAL SECTION

We used dry samples of glycerol purchased from Sigma-Aldrich ($CH_2OH−CHOH−CH_2OH$, >99.5% purity). Without additional

Received: April 4, 2017
Revised: August 1, 2017
Published: August 3, 2017

DOI: 10.1021/acs.cgd.7b00484
Cryst. Growth Des. 2017, 17, 4628−4636

purification, fresh samples were used for every experiment and were handled under nitrogen atmosphere inside a glovebag.

We explored the phase transformation of the supercooled liquid by means of dielectric spectroscopy. With this purpose, we filled a two-plate capacitor (electrodes made of brass) with 20 mm diameter and a gap of 0.25 mm controlled by a Kapton polyimide spacer. Once the capacitor was filled with the liquid material, it was transferred to the measuring cryostat and collection of the sample capacitance as a function of frequency was carried out. For a detailed description of the dielectric setup and cryostat, we refer the reader to the following publications.[16,17] From the raw data, the complex dielectric permittivity of the sample $\varepsilon^*(\omega) = \varepsilon'(\omega) - i\varepsilon''(\omega)$ is easily calculated by dividing the complex capacitance of the capacitor filled with the sample by the empty one.[18]

The procedure we used to induce the solidification of glycerol consisted of the thermal protocol depicted in Figure 1. We cooled

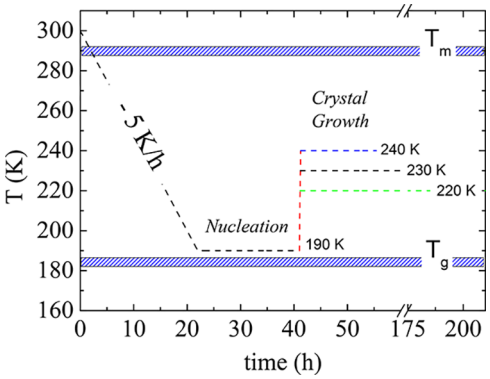

Figure 1. Thermal protocol for facilitating the transformation of liquid glycerol into the crystalline phase. Nucleation is promoted by annealing at 190 K during 19 h and crystal growth takes place at 220, 230, and 240 K. Melting and glass transition temperatures are highlighted.

down the liquid sample from 300 to 190 K at a cooling rate of approximately 5 K/h. Then, an isothermal annealing, approximately 5 K above T_g, at 190 K during 19 h was followed by a second isothermal treatment at the corresponding crystal growth temperature.

RESULTS AND DATA ANALYSIS

We have recently discussed the effect of annealing at 190 K on the dielectric signal in detail.[10] We observed a direct dependence of this annealing on the kinetics of crystal growth at higher temperatures, demonstrating the effectiveness of such annealing near the glass transition to induce the crystal nucleation. In this paper we go a step further and we explore the temperature dependence of the crystal growth kinetics. As an example, Figure 2 shows the temporal evolution of the complex dielectric permittivity of glycerol in the course of crystal growth at 220 K.

As the molecules abandon the liquid phase and attach to the surface of the growing crystalline lattice, the amplitude (dielectric strength) of the α relaxation progressively decreases. Assuming that dipole−dipole correlations do not undergo significant modifications during the crystallization process, the observed reduction in intensity of the dielectric relaxation curve can be related to an increase of crystallinity. As the crystallization proceeds, there is a concomitant reduction in density of relaxing entities which, in accordance to the theory of dielectric relaxation, must be reflected in a reduction of the dielectric strength $(\Delta\varepsilon)$ as indicated by $\Delta\varepsilon \propto \frac{\mu^2 N_d}{k_b T}$.[18] Here, μ is the molecular dipole moment, k_b is the Boltzmann constant, T

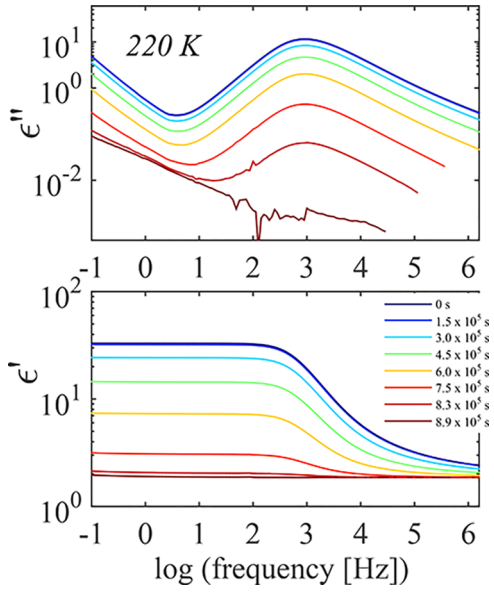

Figure 2. Complex dielectric permittivity of supercooled glycerol upon crystallization at 220 K. Imaginary (top) and real (bottom) parts of the complex permittivity are represented as a function of frequency at different stages of crystallization as indicated in the bottom panel.

is the temperature, and N_d corresponds to the total number of reorienting dipoles.

It is important to remark that the location of the α peak does not shift during the whole crystallization process. Several examples can be found in the literature in which, in the course of crystallization, there is either absence of displacement in the location of the α peak,[19,20] shifting to lower[8,21,22] or to higher[23,24] frequencies. The latter case has been interpreted from two different angles. On one side, it has been suggested that crystals would induce microscopic reorganizations of the remaining liquid that would speed up the relaxation dynamics.[25,26] Meanwhile, a macroscopic approach has been recently applied in which the displacement of the α peak toward higher frequencies is explained by Maxwell−Wagner effects in heterogeneous dielectrics.[5]

Finally, one observes the α relaxation totally vanishes. This is consistent with the formation of a fully crystallized material. With the aim of elucidating the nature of this solid phase, we heated up the sample while measuring the complex permittivity. We corroborated its crystalline nature due to the sharp increase of the dielectric permittivity around 291 K as shown in Figure 3. This temperature corresponds to the melting point of the orthorhombic structure of glycerol.[13,27]

Regarding the crystallization kinetics, as a first approach, the fraction of crystalline phase against time is related to the normalized dielectric loss α-peak intensity N, which can be calculated by means of the following expression:[7,8,10,19]

$$N(t) = \frac{\varepsilon''_{\alpha_{peak}}(0) - \varepsilon''_{\alpha_{peak}}(t)}{\varepsilon''_{\alpha_{peak}}(0) - \varepsilon''_{\alpha_{peak}}(\infty)} \quad (1)$$

where $\varepsilon''_{\alpha_{peak}}(0)$ is the value of the dielectric loss at the frequency where the α peak is located for the pure liquid, $\varepsilon''_{\alpha_{peak}}(t)$ takes the corresponding values at different crystallization times and $\varepsilon''_{\alpha_{peak}}(\infty)$ corresponds to the value of the dielectric loss at the same frequency for the pure crystal. In Figure 4, we observe that in all cases the temporal evolution of the normalized

DOI: 10.1021/acs.cgd.7b00484
Cryst. Growth Des. 2017, 17, 4628−4636

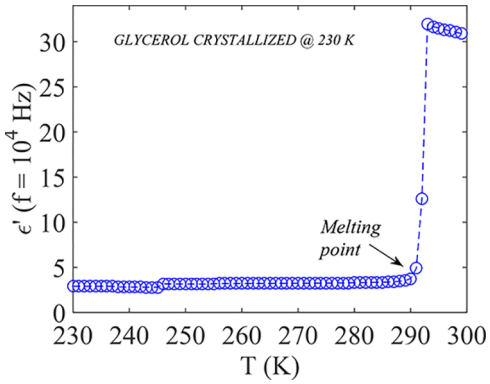

Figure 3. Real part of the dielectric permittivity at 10 kHz as a function of temperature for a sample of glycerol crystallized at 230 K. Dashed line is a guide to the eye.

dielectric loss α-peak intensity $N(t)$ shows the typical sigmoidal shape.

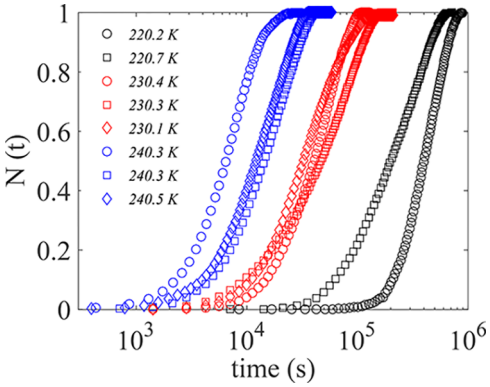

Figure 4. Time dependence of the normalized dielectric loss peak intensity (eq 1) at selected crystal growth temperatures.

Kinetics of Crystal Growth. We have analyzed the kinetics of crystal growth under the well-known Johnson–Mehl–Avrami–Kolmogorov (JMAK) model.[28−31] The JMAK model describes isothermal phase transitions that take place through nucleation and growth. Broadly speaking, this model assumes that nucleation occurs randomly from a certain number of embryos; the number of embryos decreases either by the formation of nuclei of critical size or by absorption by the growing phase; and the crystal growth rate is constant until different crystalline fronts impinge on each other. According to this model, the crystallization kinetics can be described by the following expression:

$$N(t) = 1 - \exp\left[-\left(\frac{t - t_0}{\tau_{crys}}\right)^n\right] \quad (2)$$

where τ_{crys} is the characteristic crystallization time, t_0 is the induction period, and n is the Avrami exponent, which is related to the nature of the nucleation phenomenon and dimension of the crystal growth. While, through fitting routines, one may estimate the values of the parameters that best match the experimental data, Avramov and co-workers have proposed an alternative procedure that does not require curve fitting.[15] This method uses a new set of coordinates in which the fraction of the new phase $N(t)$ is represented against $\ln(t - t_0)$. Then, the first derivative of $N(t)$ with respect to $\ln(t - t_0)$ is numerically computed. From the maximum of the first derivative curve $N'(t)$, we obtained the characteristic crystallization time and the Avrami exponent. The maximum of $N'(t)$ for the Avrami model can be derived by nullifying the second derivative of $N(t)$ with respect to $\ln(t - t_0)$, rendering the value of $N'(t)_{max} = n/e$ at $t - t_0 = \tau_{crys}$.[7,15,19] At the location of the maximum of $N'(t)$, the fraction of transformed phase $N(t)$ should take a value of 0.63, so values lower than 0.63 would indicate that $t_0 > 0$.

In Figure 5 we present the crystallization kinetics at selected temperatures and the first derivative of $N(t)$ with respect to $\ln(t$

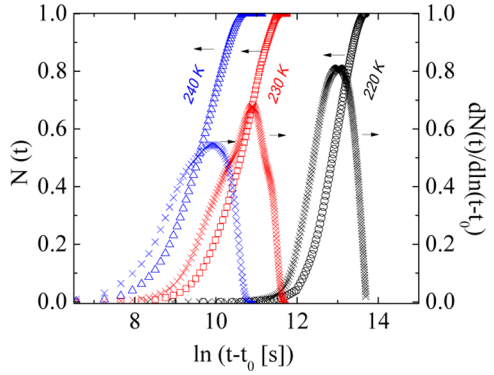

Figure 5. Evolution of the normalized dielectric loss peak intensity ($N(t)$) (open symbols) and its first derivative (×) as a function of $\ln(t - t_0)$ for crystallization processes at 220, 230, and 240 K.

$- t_0$). In all cases, the numerical differentiation gave a well resolved maximum at the characteristic crystal growth time, and only the data at 220.2 K pointed to the existence of an induction time $t_0 > 0$. To determine the value of t_0 shown in Table 1 for 220.2 K, the coordinate $\ln(t - t_0)$ is adjusted for

Table 1. Crystal Growth Kinetics Parameters of Supercooled Glycerol Obtained from the Avramov Procedure

T (K)	$\log(t_0$ [s])	n	$\log(\tau_{crys}$ [s])
220.2	3.97	2.2 ± 0.1	5.65
220.7	0	1.4 ± 0.1	5.57
230.4	0	1.8 ± 0.1	4.73
230.3	0	1.3 ± 0.1	4.90
230.1	0	1.4 ± 0.1	4.55
240.3	0	1.7 ± 0.1	3.89
240.3	0	1.5 ± 0.1	4.31
240.5	0	1.4 ± 0.1	4.27

giving a value of $N(t)$ of 0.63 coinciding with the maximum of $N'(t)$. The kinetic parameters obtained through this Avrami–Avramov plot are collected in Table 1. They show that as temperature increases the crystal growth time speeds up. Meanwhile, the values of n do not vary systematically with temperature, ranging between 2.2 and 1.3. Since we assume that crystals grow from a constant density of nuclei, it indicates that they probably grow in two dimensions.[15]

The JMAK model rationalizes isothermal crystallization kinetics, and one of the assumptions is that the crystal growth rate does not change in the course of the phase transition. But this refers to the linear growth and depending on the morphology of the growing crystals the growth rate might change in different directions. Moreover, the crystal growth rate will reduce when different crystalline fronts impinge on each

DOI: 10.1021/acs.cgd.7b00484
Cryst. Growth Des. 2017, 17, 4628−4636

other. This implies that a true physical interpretation of the resulting parameters is certainly difficult. The exponent n principally depends on the characteristics of the nucleation process and on the geometry of the growing crystals. This means that such scattering in the n values might be explained by variations in the morphology of the growing crystals that, as a consequence, will affect the rate at which they grow. Given the thermal history of the samples, where in all cases the nucleation process is induced by long annealing just above T_g, we expect the majority of nuclei already formed before the crystal growth step. Thus, the observed scattering in n is consistent with variations in the crystal growth process in such a way that we cannot know for certain that the crystal growth rate remains invariant during the whole crystallization process.

Maxwell–Wagner Analysis. In order to obtain more information about the glycerol's morphology during crystallization, we have applied the Maxwell–Wagner model for dielectric heterogeneous systems.[32] In a recent publication, Heckhser and co-workers studied systematically the crystallization of *n*-butanol at different temperatures and under different sample environments.[5] In this work, in which one of us was involved, the authors invoked Maxwell–Wagner effects to explain the peak shift toward higher frequencies and the strong reduction observed in the dielectric loss upon crystallization, in particular, for the most intense relaxation mode detected in monohydroxy alcohols.

According to the Maxwell–Wagner model, the shape and distribution of the crystals across the sample determine the resulting composite dielectric permittivity. It is important to note that the calculation of the fraction of crystalline phase as a function of time using eq 1 is based on the assumption that the dielectric permittivity of the liquid/crystal system is an additive quantity from the two domains. In case the crystal growth takes place longitudinally from one electrode to the other in discrete spots separated by gaps remaining in the liquid phase, such as we illustrate through the model A in Figure 6a, the permittivity

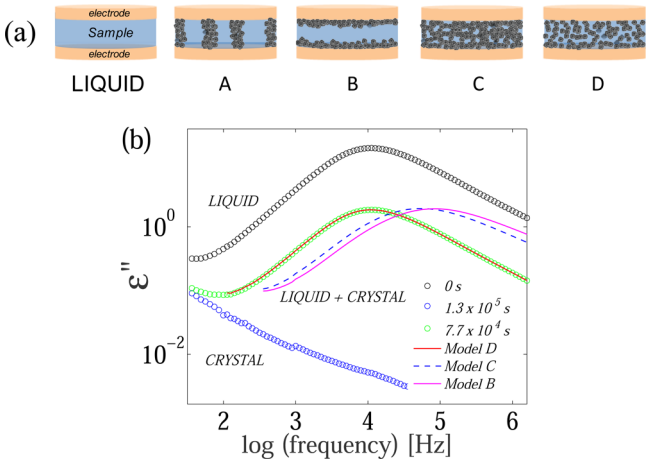

Figure 6. (a) Schematic representation of the different models we propose to illustrate the growth of the crystallites across the liquid medium. Models B, C, and D have been interpreted according to the Maxwell–Wagner model. The starting pure liquid state is also shown where sample and electrodes form a two-plate capacitor. Sample thickness is not to scale for the sake of clarity. (b) Dielectric loss as a function of frequency for the pure liquid, full crystal, and intermediate semicrystalline sample (crystallization time 7.7×10^4 s) at 230 K. The experimental data are compared to the predicted curves assuming Maxwell–Wagner effects for models B, C, and D.

of the semicrystalline material is correctly calculated by means of eq 1. On the contrary, morphologies such as the ones described in the representations B, C, and D (Figure 6a) need to be interpreted by a more realistic model. For a crystalline growth with well-defined layers parallel to the electrodes, the composite complex dielectric permittivity in terms of the Maxwell–Wagner model is expressed as follows:

$$\varepsilon^*_{\text{totalB}} = \frac{\varepsilon_c^* \varepsilon_l^*}{(1-N)\varepsilon_c^* + N\varepsilon_l^*} \tag{3}$$

where N is the volume fraction of the crystalline phase, ε_l^* is the complex permittivity of the pure liquid, and ε_c^* corresponds to the complex permittivity of the crystal phase. A more detailed description of the model can be found elsewhere.[5,18,32]

Inspired by the work reported by Heckhser and colleagues,[5] we also propose that two other models could describe the morphology of crystal growth in supercooled glycerol. In these two cases, we consider either the presence of liquid domains dispersed in a crystalline medium (model C) or crystallites dispersed in a continuous liquid phase in which percolation pathways of disordered domains persist during crystallization (model D). Using a mean-field approach the permittivity for models C and D can be quantified as[18,32,33]

$$\varepsilon^*_{\text{totalC}} = \varepsilon_c^* \frac{2\varepsilon_c^* + \varepsilon_l^* - 2(1-N)(\varepsilon_c^* - \varepsilon_l^*)}{2\varepsilon_c^* + \varepsilon_l^* + (1-N)(\varepsilon_c^* - \varepsilon_l^*)} \tag{4}$$

$$\varepsilon^*_{\text{totalD}} = \varepsilon_l^* \frac{2\varepsilon_l^* + \varepsilon_c^* - 2N(\varepsilon_l^* - \varepsilon_c^*)}{2\varepsilon_l^* + \varepsilon_c^* + N(\varepsilon_l^* - \varepsilon_c^*)} \tag{5}$$

where $1 - N$ in eq 4 corresponds to the fraction of liquid phase. The fillers embedded in the continuous matrix are assumed to be spherical and would correspond to the liquid phase and to the crystallites for models C and D respectively. It is important to remark that similar results are obtained considering fillers with other shapes, for instance, ellipsoidal.

The validity of models B, C, and D has been tested by calculating the total permittivity using the experimental values of ε_l^* and ε_c^*. The significant shift of the α peak toward higher frequencies for models B and C seen in Figure 6 allows us to discard both a layer-like crystalline front from the electrodes and a dispersion of discrete liquid droplets in a continuous crystalline medium. Much better agreement with the experimental data is found for model D. It is therefore plausible to state that the two models which best fit the raw data correspond to A and D. Accordingly, we have also estimated the crystalline amount by fitting eq 5 to the raw data. Selected snapshots of this fitting are presented in Figure 7, together with the dependence of the crystalline volume fraction as a function of the dielectric strength for models A and D. Let us note that model A does not imply Maxwell–Wagner effects, and the amount of solid phase over time is calculated by eq 1. Nevertheless, the inset in Figure 7 shows that models A and D give similar results that only differ by up to a 10% at the intermediate steps of the phase transition. In order to unravel this discrepancy, it would be of great help to use diffraction methods coupled simultaneously with relaxation techniques.[23,34]

Coupling between Molecular Mobility and Crystal Growth Kinetics. Along with the thermodynamic barrier to nucleation and crystal growth, the molecular mobility controls the rate at which the crystallization takes place.[35] Near the glass

DOI: 10.1021/acs.cgd.7b00484
Cryst. Growth Des. 2017, 17, 4628–4636

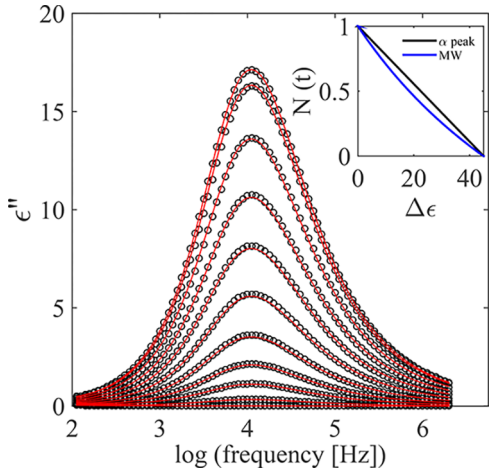

Figure 7. Fit of eq 5 (red solid lines) to the experimental data (○) during the transformation of liquid glycerol into the crystalline phase at 230 K. Crystallization time advances from top to bottom. Snapshots every 3 h approximately. The inset displays the evolution of the crystalline volume fraction as a function of the dielectric strength according to models A (linear combination of amorphous and crystalline domains, eq 1) and D (Maxwell–Wagner effect, eq 5).

transition, the transport of molecular entities across the liquid–crystal interface is generally identified to be the bottleneck for the overall crystallization process.[9,36,37] Moreover, it has been widely debated what dynamic feature mainly couples with the crystallization kinetics.[7,35,38] Here, by controlling temperature, we explored the correlation of the crystal growth rate with the structural α relaxation.

Figure 8 shows the acceleration of the kinetics of crystal growth in supercooled liquid glycerol as the temperature

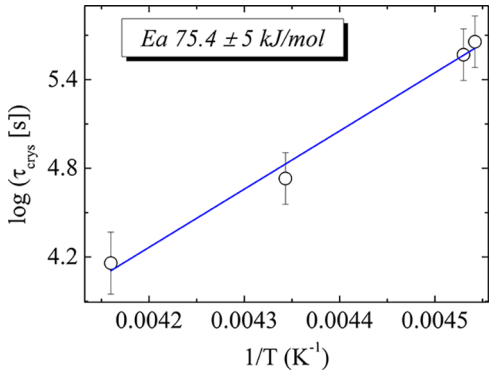

Figure 8. Characteristic crystallization time against reciprocal temperature. Solid line represents the fit of the experimental data to the Arrhenius equation $\tau_{crys} = \tau_0 \exp\left(\frac{E_a}{RT}\right)$. Here, E_a is an activation energy, R is the gas constant, and τ_0 is a pre-exponential factor with ps time scale.

increases. In agreement with what we show here, several groups have reported that near T_g, the crystallization of liquid glycerol slows down as the temperature decreases,[12,14] which, leaving aside a possible variation of the thermodynamic driving force with temperature, indicates a direct coupling between mobility and crystal growth. The error bars in Figure 8 were defined by the upper and lower limits with respect to the average value obtained from three different measurements both at 230 and 240 K. Given the actual temperature (estimated from the location of the α-peak) of these sets of measurements was very similar, we decided to group them and calculate the average and the corresponding limits of confidence. In contrast, between the two points at low temperatures, 220.2 and 220.7 K, the gap in frequency of the maximum loss for the α-peak was too large (consequence of the dynamic fragility) to consider these two temperatures as equivalent. This is why for these two low temperature measurements we did not have the possibility of averaging several crystallization times for getting the corresponding error bar. Nevertheless, at low temperature we expect less uncertainty in the characteristic crystallization times given the much slower kinetics as the temperature approaches T_g. In any case, we assume that the error bar for the low temperature measurements is equivalent to the one shown by the 230 K data. The linearity observed in Figure 8 allowed us to calculate an activation barrier (E_a = 75.4 kJ/mol and $\tau_0 \approx 1$ ps) by means of the Arrhenius law. In order to assign a physical meaning to this activation barrier, we emphasize the thermal history of the sample. Given that the nucleation step mainly took place during the preannealing at 190 K, it seems plausible to assume that crystals grew from an almost constant density of pre-existing nuclei. Therefore, despite the fact that, in general, the overall crystallization time depends on both nucleation and growth, here we report data that are mostly associated with the crystal growth part. In this scenario and under the framework of the JMAK model, the crystallization time τ_{crys} is inversely proportional to the crystal growth rate U ($\tau_{crys} \propto \frac{1}{U}$).[15]

DISCUSSION

Our results indicate that glycerol crystallizes into the standard orthorhombic phase with a crystal growth kinetics that slows down as the temperature approaches T_g. Taking into account the thermal history of the sample and the combination of results from the Avramov and Maxwell–Wagner analyses, glycerol's crystals probably grow as spherical or disc-shape particles homogeneously distributed across the liquid matrix, along with some planar growth fronts.

Numerous studies have recently focused on the microscopic origin of metastable phases formed in the supercooled regime, normally characterized by distinct structural, dynamic, and thermodynamic properties to those of the supercooled liquid and crystalline phases.[39−41] The transformation of supercooled liquids into solid glacial phases or the existence of liquid–liquid transitions has been proposed in a great variety of systems, from pure inorganic liquids to water. As a general feature, these liquids show the ability to create locally favored aggregates cooperatively.[42] The formation of these locally favored structures competes against crystallization and has been predicted by the theory of frustration-limited domains.[43] Whether or not these locally favored structures are behind the origin of the so-called glacial phase in systems, such as *n*-butanol and tryphenyl phosphite, is still a matter of debate.[5,40,43,44] Our data do not support that liquid glycerol transforms into a glacial or partially disordered phase. By careful control of the experimental conditions and preparing always the sample following the same protocol, we have tried to minimize as much as possible external effects on the sample behavior that could compromise the reproducibility of the presented results. As we have reported in a recent publication, we only observed a rare event in which the glycerol's crystallization was aborted at the very late stages.[10] We therefore believe that, in the case that glycerol formed a glacial

DOI: 10.1021/acs.cgd.7b00484
Cryst. Growth Des. 2017, 17, 4628−4636

phase, it would simply be the result of the frustration of the growing of the standard orthorhombic lattice.

A great effort has been recently done to disentangle the distinct role played by dynamics and thermodynamics during nucleation and crystal growth.[3,45] As we have mentioned before, the experimental protocol we used to force glycerol to crystallize is consistent with the formation of crystals that grow mainly from pre-existing nuclei. According to the classical theory of crystallization,[3,46−51] the characteristic time of crystal growth can be simplified as

$$\tau_{\mathrm{crys}}(T) = \frac{A}{\left[1 - \exp\left(-\frac{\Delta G(T)}{k_{\mathrm{b}}T}\right)\right]\exp\left(-\frac{\Delta E(T)}{k_{\mathrm{b}}T}\right)} \quad (6)$$

where A is a factor that depends on the type of crystal growth mechanism and the density of crystal nuclei, ΔG is the thermodynamic driving force, and ΔE is the activation energy for transport across the liquid/crystal interface. ΔE, whose maximum value is normally reached near T_{g}, governs the short distance diffusion of the crystallizing elements across the phase boundary and is therefore determined by the self-diffusion coefficient. The kinetic contribution to the crystal growth rate (second exponential in eq 6) is explicitly modulated by a scale factor which accounts for the probability that a molecule has the proper conformation to be accommodated onto the crystalline surface.

We do not monitor the self-diffusion coefficient directly, but a related property, namely, the dielectric α relaxation time. The Debye model predicts the following proportionality between viscosity η and α relaxation time τ_α:[52,53]

$$\frac{1}{\tau_\alpha} = \frac{2k_{\mathrm{b}}T}{8\pi r^3 \eta} \quad (7)$$

being r a hydrodynamic radius. Known as Debye−Stokes−Einstein (DSE), this relation holds to a certain degree in glycerol for large variations in τ_α and η.[54] In Figure 9 we compare both our dielectric τ_α and the viscosity data extracted from the article by Schröter and Donth[54] with the crystal growth time τ_{crys}. We observe almost the same correlation. The coupling coefficient is quantified as the slope of the linear dependence of $\log(\tau_\alpha)$ or $\log(\eta)$ with $\log(\tau_{\mathrm{crys}})$.[2,7] The linear fits in Figure 9 yield coupling coefficients with values of 0.75 and 0.74 for τ_α and viscosity respectively, revealing a connection between the structural relaxation time (viscosity) and the kinetics of crystal growth. Typically, in organic molecular liquids the coupling coefficient takes values between 0.3 and 0.9.[1,2,7,38,55−57]

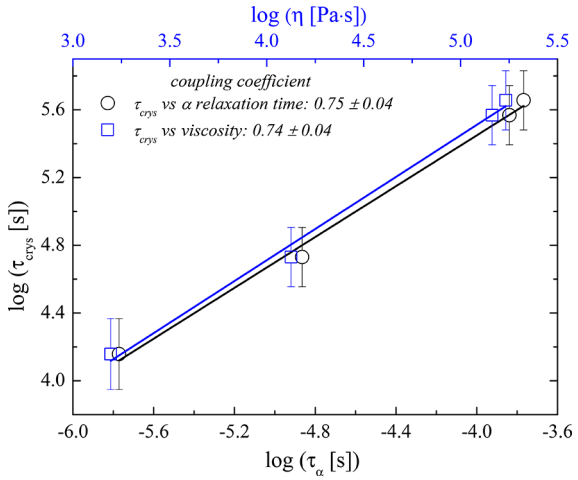

Figure 9. Evolution of the characteristic crystallization time on a double x-axes representation against τ_α (α relaxation time) and shear viscosity (data from ref 54). Solid lines represent linear fits.

The extent to which the crystal growth rate decouples from viscosity was empirically correlated with the dynamic fragility in both organic and inorganic systems by Ediger and co-workers.[2] It was proposed that the coupling coefficient ξ and fragility m are related by the following linear dependence $\xi = 1.1 - 0.005m$.[2] Our coupling coefficient matches reasonably well with this expression since the predicted value is around 14% higher than the observed one shown in Figure 9. For this estimation we have used an isobaric fragility index of 48.[10] This interrelationship indicates that the decoupling between viscosity and crystal growth rate is principally due to the intrinsic nature of the liquid relaxation. Similarly, a connection between the dynamic fragility and the crystalline nucleation rate was postulated for polymeric systems.[9]

However, considering that in the classical picture of crystal growth, molecular diffusion is behind the energy barrier to transport of molecules across the phase boundary (second exponential of eq 6), we expect a deeper correlation between τ_{crys} and self-diffusion coefficient in comparison to τ_α or η. With this purpose, we have estimated the self-diffusion coefficient of glycerol by means of the fractional Stokes−Einstein relation:

$$D = \frac{k_{\mathrm{b}}T}{6\pi r \eta^{\gamma}} \quad (8)$$

To compute the values of D, we have used the shear viscosity data by Schröter and Donth[54] and the hydrodynamic radius (0.145 nm) reported by Chen and co-workers.[58] The fractional exponent γ in eq 8 determines the decoupling between viscosity and diffusion (violation of the Stokes−Einstein relation) normally observed in viscous liquids near T_{g}. By NMR experiments, Mallamace et al. have recently found that γ takes a constant value of 0.85 in water−glycerol mixtures in a wide range of compositions.[59] In fact, these authors argue that this value of 0.85 shows a universal character in a broad spectrum of liquids, although different values can be found in the literature.[38,60,61] By using $\gamma = 0.85$, in Figure 10 we show the evolution of the characteristic crystal growth time as a function of the self-diffusion coefficient for pure glycerol. The coupling coefficient now takes a value of −0.85 as indicated by the slope of $\log(\tau_{\mathrm{crys}})$ vs $\log(D)$. We must stress that for glycerol the experimental values of D are unknown in our temperature range of interest. Thus, we assume the reported fractional exponent that relates viscosity with diffusion as $D \propto \eta^{-0.85}$ also holds between 220 and 240 K.

The correlation between τ_{crys} and D is even stronger when the observed data are corrected for the thermodynamic component of eq 6. Thus, by multiplying the observed τ_{crys} by $\left[1 - \exp\left(-\frac{\Delta G(T)}{k_{\mathrm{b}}T}\right)\right]$, the kinetic part of the crystal growth time is derived.[2] It is commonly assumed that the Gibbs free energy difference between the crystal and liquid phases $\Delta G(T)$ can be rewritten as the product of the corresponding entropy difference at the melting point ΔS_{m}[62,63] and the undercooling ΔT.[2,3,35] In this way, the kinetic part of the characteristic crystal growth time τ^*_{crys} is given by

DOI: 10.1021/acs.cgd.7b00484
Cryst. Growth Des. 2017, 17, 4628−4636

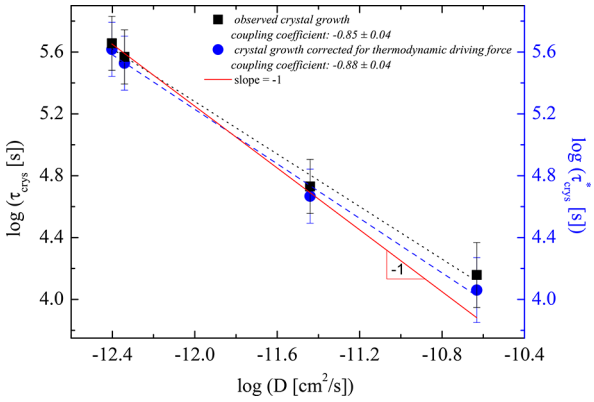

Figure 10. Experimentally observed crystal growth time as a function of the estimated self-diffusion coefficient (eq 8). The graph also displays the crystal growth time corrected for the thermodynamic driving force (eq 9). Dotted and dashed lines correspond to the linear fits of the observed and corrected data, respectively. The red solid line represents an scaling with slope −1 as a reference.

$$\tau^*_{crys}(T) = \tau_{crys}\left[1 - \exp\left(-\frac{\Delta S_m \Delta T}{k_b T}\right)\right] \quad (9)$$

In Figure 10, we see that $\log(\tau^*_{crys})$ also shows a linear dependence with $\log(D)$, whose slope is −0.88. It is worth noting that, as temperature decreases, the kinetic part of the crystal growth rate converges with the observed values, corroborating that near T_g the thermodynamic driving force has less and less influence on the kinetics of crystal growth. Even though we demonstrate that the thermodynamic driving force slightly varies during our explored temperature range, it is important to note that the factor A in eq 6 could be temperature-dependent. For flat liquid/crystal interfaces that growth laterally, A depends on both the thermodynamic driving force and the surface tension of the liquid/crystal interface. According to Jackson[64] and due to its high entropy of melting ($\Delta S_m > 4R$),[2] glycerol is expected to show a flat liquid/crystal interface growing laterally either by screw dislocation or surface nucleation growth.[3,49] Given this specific mechanism of crystal growth expected for glycerol, the term A probably varies over the temperature range explored. Therefore, along with other variables discussed above, this reasoning might explain the departure from a full correlation between self-diffusion coefficient and crystal growth time revealed in the present paper.

Regarding the poor crystallization ability of supercooled glycerol, different arguments proposed that a high value of ΔS_m hinders the tendency to crystallize. On one side, the probability that a liquid fluctuation fails to accommodate properly onto the surface of the growing crystal is higher the more ordered the crystal is with respect to the bulk liquid.[2,65] On the other side, at least for atomic systems, it was suggested that the interfacial free energy is directly proportional to the entropy of melting.[3,66] Because of the distinct impact of the interfacial free energy on the kinetics of nucleation and growth, a large value of the surface tension increases the temperature gap between the maximum of nucleation and growth rates, in such a way the crystallization process takes places less easily.

In spite of its poor crystallization ability, we demonstrate that glycerol does not form solid structures resembling those created in glacial phases, at least on a regular basis in the temperature range explored here.

CONCLUSION

An appropriate thermal protocol allowed us to control the nucleation and crystal growth in glycerol near T_g. Our results are consistent with the transformation of liquid glycerol into the standard orthorhombic state, and we do not find any evidence suggesting that it transforms into a peculiar solid phase with distinct structural or mechanical properties. As we have recently reported,[10] in one single case we observed a rare event in which the transformation into the crystalline state was frustrated at the very late stages. A subtle balance between kinetic and thermodynamic effects may explain the occurrence of sporadic aborted crystal growth phenomena with total lack of reproducibility.[39] The existence of glycerol's solid phases with lower values of the shear modulus than that for the standard crystalline phase as reported by Möbius and colleagues[12] could be explained by these random aborted crystallization processes.

We have also determined a strong dependence of the molecular mobility in the kinetics of crystal growth. We find a scaling exponent of −0.85 when the characteristic crystal growth time is plotted against the self-diffusion coefficient in a log−log representation. A perfect coupling between crystal growth time and diffusion would render values of the coupling coefficient very close to −1.

We did not study the crystallization at low temperatures, that is, below $1.19T_g$. It therefore remains a possibility that the frustrated crystalline phase could form with higher reproducibility in this range. However, it is worthy to remark that the transformation of liquid glycerol into the crystalline phase below $1.19T_g$ is expected to be completed after extremely long waiting times. Nonetheless, dielectric and/or diffraction experiments on the whole crystallization process in deeply supercooled glycerol will be certainly of future interest.

We must also stress that our conclusions could be slightly altered in case these experiments were repeated in different sample environments. We have already mentioned that crystallization is a complex phenomenon in which many factors play a simultaneous role, including the physical interaction between sample and container which could make samples exhibit a different behavior.[5] Exploring the crystallization of glycerol samples enclosed by different kind of containers is an interesting avenue for future research.

One limitation of dielectric spectroscopy is that it only provides indirect information on the structural development. To overcome this drawback and obtain a full picture of glycerol's crystallization from structural and dynamic points of view, in future studies we propose the utilization of the combined neutron diffraction-dielectrics cell developed by one the authors which was successfully employed for crystallization studies in monohydroxy alcohols.[23,25,34,67]

In summary, supercooled glycerol transforms into the crystalline state via nucleation and crystal growth without significant modifications of the structural dynamics in the remaining liquid phase during the whole process.[10] Moreover, we now show evidence of the relation between different dynamic properties of the bulk liquid (relaxation time, viscosity and diffusion) and the kinetics of crystal growth. There is not a perfect correlation between the self-diffusion coefficient and the characteristic time of crystal growth, even when the observed values are corrected from the thermodynamic contribution, although several arguments have been presented above that could explain this. Nevertheless, the data we show here indicate that molecular mobility of glycerol, not solely, is the principal

DOI: 10.1021/acs.cgd.7b00484
Cryst. Growth Des. 2017, 17, 4628−4636

factor governing its crystal growth above but close to T_g. Given the information we reveal about the dynamics−structure interrelationships during nucleation and crystal growth, the implications of our study are mainly related to fundamental and practical questions of the crystallization phenomenon. Moreover, our research also offers new insights about the liquid's dynamics of one the most archetypal glass-forming systems.

AUTHOR INFORMATION

Corresponding Author

*E-mail: asanz@ruc.dk.

ORCID

Alejandro Sanz: 0000-0001-5103-4049

Notes

The authors declare no competing financial interest.

ACKNOWLEDGMENTS

This work has been funded by the Danish Council for Independent Research (Sapere Aude: Starting Grant). Technical support from the workshop at IMFUFA (Department of Science and Environment, Roskilde University) is also acknowledged.

REFERENCES

(1) Adrjanowicz, K.; Koperwas, K.; Szklarz, G.; Tarnacka, M.; Paluch, M. Exploring the Crystallization Tendency of Glass-Forming Liquid Indomethacin in the T − p Plane by Finding Different Iso-Invariant Points. *Cryst. Growth Des.* **2016**, *16*, 7000−7010.

(2) Ediger, M. D.; Harrowell, P.; Yu, L. Crystal growth kinetics exhibit a fragility-dependent decoupling from viscosity. *J. Chem. Phys.* **2008**, *128*, 034709.

(3) Descamps, M.; Dudognon, E. Crystallization from the Amorphous State: Nucleation − Growth Decoupling, Polymorphism Interplay, and the Role of Interfaces. *J. Pharm. Sci.* **2014**, *103*, 2615−2628.

(4) Ryabov, Y.; Hayashi, Y.; Gutina, A.; Feldman, Y. Features of supercooled glycerol dynamics. *Phys. Rev. B: Condens. Matter Mater. Phys.* **2004**, *69*, 189904.

(5) Jensen, M. H.; Alba-Simionesco, C.; Niss, K.; Hecksher, T. A systematic study of the isothermal crystallization of the mono-alcohol n-butanol monitored by dielectric spectroscopy. *J. Chem. Phys.* **2015**, *143*, 134501.

(6) Koperwas, K.; Adrjanowicz, K.; Wojnarowska, Z.; Jedrzejowska, A.; Knapik, J.; Paluch, M. Glass-Forming Tendency of Molecular Liquids and the Strength of the Intermolecular Attractions. *Sci. Rep.* **2016**, *6*, 36934.

(7) Kolodziejczyk, K.; Paluch, M.; Grzybowska, K.; Grzybowski, A.; Wojnarowska, Z.; Hawelek, L.; Ziolo, J. D. Relaxation Dynamics and Crystallization Study of Sildenafil in the Liquid and Glassy States. *Mol. Pharmaceutics* **2013**, *10*, 2270−2282.

(8) Viciosa, M. T.; Correia, N. T.; Sánchez, M. S.; Carvalho, A. L.; Romão, M. J.; Gómez Ribelles, J. L.; Dionísio, M. Real-Time Monitoring of Molecular Dynamics of Ethylene Glycol Dimethacrylate Glass Former. *J. Phys. Chem. B* **2009**, *113*, 14209−14217.

(9) Sanz, A.; Nogales, A.; Ezquerra, T. A. Influence of Fragility on Polymer Cold Crystallization. *Macromolecules* **2010**, *43*, 29−32.

(10) Sanz, A.; Niss, K. Liquid dynamics in partially crystalline glycerol. *J. Chem. Phys.* **2017**, *146*, 044502.

(11) Zondervan, R.; Xia, T.; van der Meer, H.; Storm, C.; Kulzer, F.; van Saarloos, W.; Orrit, M. Soft glassy rheology of supercooled molecular liquids. *Proc. Natl. Acad. Sci. U. S. A.* **2008**, *105*, 4993−4998.

(12) Möbius, M. E.; Xia, T.; van Saarloos, W.; Orrit, M.; van Hecke, M. Aging and Solidification of Supercooled Glycerol. *J. Phys. Chem. B* **2010**, *114*, 7439−7444.

(13) Bermejo, F. J.; Criado, A.; de Andres, A.; Enciso, E.; Schober, H. Microscopic dynamics of glycerol in its crystalline and glassy states. *Phys. Rev. B: Condens. Matter Mater. Phys.* **1996**, *53*, 5259−5267.

(14) Yuan, H.-F.; Xia, T.; Plazanet, M.; Demé, B.; Orrit, M. Crystallite nucleation in supercooled glycerol near the glass transition. *J. Chem. Phys.* **2012**, *136*, 041102.

(15) Avramov, I.; Avramova, K.; Russel, C. New method to analyze data on overall crystallization kinetics. *J. Cryst. Growth* **2005**, *285*, 394−399.

(16) Igarashi, B.; Christensen, T.; Larsen, E. H.; Olsen, N. B.; Pedersen, I. H.; Rasmussen, T.; Dyre, J. C. An impedance-measurement setup optimized for measuring relaxations of glass-forming liquids. *Rev. Sci. Instrum.* **2008**, *79*, 045106.

(17) Igarashi, B.; Christensen, T.; Larsen, E. H.; Olsen, N. B.; Pedersen, I. H.; Rasmussen, T.; Dyre, J. C. A cryostat and temperature control system optimized for measuring relaxations of glass-forming liquids. *Rev. Sci. Instrum.* **2008**, *79*, 045105.

(18) Schönhals, A.; Kremer, F. *Broadband Dielectric Spectroscopy*; Springer-Verlag: Berlin Heidelberg, 2003.

(19) Napolitano, S.; Wubbenhorst, M. Monitoring the cold crystallization of poly(3-hydroxy butyrate) via dielectric spectroscopy. *J. Non-Cryst. Solids* **2007**, *353*, 4357−4361.

(20) Alie, J.; Menegotto, J.; Cardon, P.; Duplaa, H.; Caron, A.; Lacabanne, C.; Bauer, M. Dielectric study of the molecular mobility and the isothermal crystallization kinetics of an amorphous pharmaceutical drug substance. *J. Pharm. Sci.* **2004**, *93*, 218−233.

(21) Dobbertin, J.; Hannemann, J.; Schick, C.; Pötter, M.; Dehne, H. Molecular dynamics of the α-relaxation during crystallization of a low-molecular-weight compound: A real-time dielectric spectroscopy study. *J. Chem. Phys.* **1998**, *108*, 9062−9068.

(22) Nogales, A.; Ezquerra, T.; Denchev, Z.; Sics, I.; Baltá Calleja, F. J.; Hsiao, B. Molecular dynamics and microstructure development during cold crystallization in poly(ether-ether-ketone) as revealed by real time dielectric and X-ray methods. *J. Chem. Phys.* **2001**, *115*, 3804−3813.

(23) Sanz, A.; Nogales, A.; Puente-Orench, I.; Jiménez-Ruiz, M.; Ezquerra, T. A. Changes in mobility of plastic crystal ethanol during its transformation into the monoclinic crystal state. *J. Chem. Phys.* **2014**, *140*, 054510.

(24) Adrjanowicz, K.; Kaminski, K.; Wojnarowska, Z.; Dulski, M.; Hawelek, L.; Pawlus, S.; Paluch, M.; Sawicki, W. Dielectric Relaxation and Crystallization Kinetics of Ibuprofen at Ambient and Elevated Pressure. *J. Phys. Chem. B* **2010**, *114*, 6579−6593.

(25) Sanz, A.; Jiménez-Ruiz, M.; Nogales, A.; Martín y Marero, D.; Ezquerra, T. Hydrogen-bond network breakage as a first step to isopropanol crystallization. *Phys. Rev. Lett.* **2004**, *93*, 015503.

(26) Tripathi, P.; Romanini, M.; Tamarit, J. L.; Macovez, R. Collective relaxation dynamics and crystallization kinetics of the amorphous Biclotymol antiseptic. *Int. J. Pharm.* **2015**, *495*, 420−427.

(27) Cuello, G. J.; Bermejo, F. J.; Fayos, R.; Fernández-Perea, R.; Criado, A.; Trouw, F.; Tam, C.; Schober, H.; Enciso, E.; Almarza, N. G. Anharmonic dynamics in crystalline, glassy, and supercooled-liquid glycerol: A case study on the onset of relaxational behavior. *Phys. Rev. B: Condens. Matter Mater. Phys.* **1998**, *57*, 8254−8263.

(28) Kolmogorov, A. *Izv. Akad. Nank. SSSR* **1937**, *3*, 355.

(29) Johnson, W.; Mehl, R. Reaction kinetics in processes of nucleation and growth. *Trans. Am. Inst. Mining Metall. Eng.* **1939**, *135*, 416−442.

(30) Avrami, M. Kinetics of phase change. I General theory. *J. Chem. Phys.* **1939**, *7*, 1103−1112.

(31) Avrami, M. Kinetics of phase change. II Transformation − Time Relations for Random Distribution of Nuclei. *J. Chem. Phys.* **1940**, *8*, 212.

(32) Richert, R. Dielectric spectroscopy and dynamics in confinement. *Eur. Phys. J.: Spec. Top.* **2010**, *189*, 37−46.

(33) Wagner, K. W. *Arch. Elektrotech.* **1914**, *2*, 371.

(34) Jiménez-Ruiz, M.; Sanz, A.; Nogales, A.; Ezquerra, T. Experimental setup for simultaneous measurements of neutron

DOI: 10.1021/acs.cgd.7b00484
Cryst. Growth Des. 2017, 17, 4628−4636

diffraction and dielectric spectroscopy during crystallization of liquids. *Rev. Sci. Instrum.* **2005**, *76*, 043901.
(35) Adrjanowicz, K.; Grzybowski, A.; Grzybowska, K.; Pionteck, J.; Paluch, M. Toward Better Understanding Crystallization of Supercooled Liquids under Compression: Isochronal Crystallization Kinetics Approach. *Cryst. Growth Des.* **2013**, *13*, 4648−4654.
(36) Turnbull, D.; Fisher, J. Rate of Nucleation in Condensed Systems. *J. Chem. Phys.* **1949**, *17*, 71−73.
(37) Fokin, V. M.; Zanotto, E. D.; Yuritsyn, N. S.; Schmelzer, J. W. P. Homogeneous crystal nucleation in silicate glasses: A 40 years perspective. *J. Non-Cryst. Solids* **2006**, *352*, 2681−2714.
(38) Swallen, S. F.; Ediger, M. D. Self-diffusion of the amorphous pharmaceutical indomethacin near T-g. *Soft Matter* **2011**, *7*, 10339−10344.
(39) Demirjian, B. G.; Dosseh, G.; Chauty, A.; Ferrer, M.-L.; Morineau, D.; Lawrence, C.; Takeda, K.; Kivelson, D.; Brown, S. Metastable Solid Phase at the Crystalline-Amorphous Border: The Glacial Phase of Triphenyl Phosphite. *J. Phys. Chem. B* **2001**, *105*, 2107−2116.
(40) Shmyt'ko, I. M.; Jiménez-Riobóo, R. J.; Hassaine, M.; Ramos, M. A. Structural and thermodynamic studies of n-butanol. *J. Phys.: Condens. Matter* **2010**, *22*, 195102.
(41) Murata, K.; Tanaka, H. Liquid − liquid transition without macroscopic phase separation in a water-glycerol mixture. *Nat. Mater.* **2012**, *11*, 436−443.
(42) Poole, P.; Grande, T.; Angell, C.; McMillan, P. Polymorphic phase transitions in liquids and glasses. *Science* **1997**, *275*, 322−323.
(43) Kivelson, D.; Kivelson, S.; Zhao, X.; Nussinov, Z.; Tarjus, G. A thermodynamic theory of supercooled liquids. *Phys. A* **1995**, *219*, 27−38.
(44) Hedoux, A.; Guinet, Y.; Descamps, M.; Benabou, A. Raman scattering investigation of the glaciation process in triphenyl phosphite. *J. Phys. Chem. B* **2000**, *104*, 11774−11780.
(45) Adrjanowicz, K.; Grzybowski, A.; Grzybowska, K.; Pionteck, J.; Paluch, M. Effect of High Pressure on Crystallization Kinetics of van der Waals Liquid: An Experimental and Theoretical Study. *Cryst. Growth Des.* **2014**, *14*, 2097−2104.
(46) Wilson, H. XX. On the velocity of solidification and viscosity of super-cooled liquids. *Philosophical Magazine Series 5* **1900**, *50*, 238−250.
(47) Frenkel, J. *Phys. Z. Sowjet Union* **1932**, *1*, 498.
(48) Turnbull, D. In *Solid State Physics*; Seitz, F., Turnbull, D., Eds.; Solid State Physics; Academic Press, 1956; Vol. 3, pp 225−306.
(49) Gutzow, I. Mechanism of crystal-growth in glass forming systems. *J. Cryst. Growth* **1977**, *42*, 15−23.
(50) Schmelzer, J. W.; Zanotto, E. D.; Avramov, I.; Fokin, V. M. Stress development and relaxation during crystal growth in glass-forming liquids. *J. Non-Cryst. Solids* **2006**, *352*, 434−443.
(51) Adrjanowicz, K.; Kaminski, K.; Paluch, M.; Niss, K. Crystallization Behavior and Relaxation Dynamics of Supercooled S-Ketoprofen and the Racemic Mixture along an Isochrone. *Cryst. Growth Des.* **2015**, *15*, 3257−3263.
(52) Debye, P.; Falkenhagen, H. Dispersion of conductability and dielectricity constants of strong electrolytes. *Physik. Z.* **1928**, *29*, 401−426.
(53) Debye, P. *Polar Liquids*; The Chemical Catalog Company, Inc, 1929.
(54) Schröter, K.; Donth, E. Viscosity and shear response at the dynamic glass transition of glycerol. *J. Chem. Phys.* **2000**, *113*, 9101−9108.
(55) Zhou, D.; Zhang, G. G. Z.; Law, D.; Grant, D. J. W.; Schmitt, E. A. Thermodynamics, Molecular Mobility and Crystallization Kinetics of Amorphous Griseofulvin. *Mol. Pharmaceutics* **2008**, *5*, 927−936.
(56) Bhardwaj, S. P.; Arora, K. K.; Kwong, E.; Templeton, A.; Clas, S.-D.; Suryanarayanan, R. Correlation between Molecular Mobility and Physical Stability of Amorphous Itraconazole. *Mol. Pharmaceutics* **2013**, *10*, 694−700.
(57) Korhonen, O.; Bhugra, C.; Pikal, M. J. Correlation between molecular mobility and crystal growth of amorphous phenobarbital and phenobarbital with polyvinylpyrrolidone and L-proline. *J. Pharm. Sci.* **2008**, *97*, 3830−3841.
(58) Chen, B.; Sigmund, E. E.; Halperin, W. P. Stokes-Einstein Relation in Supercooled Aqueous Solutions of Glycerol. *Phys. Rev. Lett.* **2006**, *96*, 145502.
(59) Mallamace, F.; Corsaro, C.; Mallamace, D.; Vasi, S.; Vasi, C.; Stanley, H. E. Some considerations on the transport properties of water-glycerol suspensions. *J. Chem. Phys.* **2016**, *144*, 014501.
(60) Adrjanowicz, K.; Kaminski, K.; Tarnacka, M.; Szutkowski, K.; Popenda, L.; Bartkowiak, G.; Paluch, M. The effect of hydrogen bonding propensity and enantiomeric composition on the dynamics of supercooled ketoprofen - dielectric, rheological and NMR studies. *Phys. Chem. Chem. Phys.* **2016**, *18*, 10585−10593.
(61) Swallen, S. F.; Bonvallet, P. A.; McMahon, R. J.; Ediger, M. D. Self-Diffusion of tris-Naphthylbenzene near the Glass Transition Temperature. *Phys. Rev. Lett.* **2003**, *90*, 015901.
(62) Gibson, G.; Giauque, W. The third law of thermodynamics evidence from the specific heats of glycerol that the entropy of a glass exceeds that of a crystal at the absolute zero. *J. Am. Chem. Soc.* **1923**, *45*, 93−104.
(63) Ediger, M.; Angell, C.; Nagel, S. Supercooled liquids and glasses. *J. Phys. Chem.* **1996**, *100*, 13200−13212.
(64) Jackson, K. *Kinetic Processes*; Wiley-VCH: Weinheim, 2004.
(65) Burke, E.; Broughton, J. Q.; Gilmer, G. H. Crystallization of fcc (111) and (100) crystal-melt interfaces: A comparison by molecular dynamics for the Lennard-Jones system. *J. Chem. Phys.* **1988**, *89*, 1030−1041.
(66) Spaepen, F. Structural model for solid-liquid interface in monatomic systems. *Acta Metall.* **1975**, *23*, 729−743.
(67) Sanz, A.; Nogales, A.; Puente-Orench, I.; Jiménez-Ruiz, M.; Ezquerra, T. A. Detection of Early Stage Precursor during Formation of Plastic Crystal Ethanol from the Supercooled Liquid State: A Simultaneous Dielectric Spectroscopy with Neutron Diffraction Study. *Phys. Rev. Lett.* **2011**, *107*, 025502.

DOI: 10.1021/acs.cgd.7b00484
Cryst. Growth Des. 2017, 17, 4628−4636